THE JOURNAL OF BIOLOGICAL CHEMISTRY VOL. 282, NO. 10, pp. 6992–7000, March 9, 2007

A Histidine-rich Cluster Mediates the Ubiquitination and Degradation of the Human Zinc Transporter, hZIP4, and Protects against Zinc Cytotoxicity*

Received for publication, November 13, 2006, and in revised form, December 13, 2006 Published, JBC Papers in Press, January 3, 2007, DOI 10.1074/jbc.M610552200

Xiaoqing Mao[‡1], **Byung-Eun Kim**[‡1], **Fudi Wang**[‡], **David J. Eide**[§], **and Michael J. Petris**[‡2]

From the [‡]*Departments of Biochemistry and Nutritional Sciences, University of Missouri, Columbia, Missouri 65211 and the* [§]*Department of Nutritional Sciences, University of Wisconsin, Madison, Wisconsin 53706*

Zinc is an essential nutrient. Genetic evidence for this nutritional requirement in humans is the zinc deficiency disease, acrodermatitis enteropathica. This disorder is caused by mutations in hZIP4 (*SLC39A4*), a zinc importer required for zinc uptake in enterocytes and other cell types. Studies in mice have demonstrated that levels of the mZIP4 mRNA are reduced by elevated dietary zinc, resulting in a decreased abundance of the ZIP4 protein at the plasma membrane. Moreover, studies in cultured cells have demonstrated that low micromolar concentrations of zinc stimulate the endocytosis of the mZIP4 protein resulting in a reduction in cellular zinc uptake. In this study, we demonstrate an additional level of hZIP4 regulation involving ubiquitination and degradation of this transporter in elevated zinc concentrations. Mutational analysis identified a cytoplasmic histidine-rich domain that was essential for ubiquitin-dependent degradation of ZIP4 and protection against zinc toxicity. However, this motif was dispensable for zinc-induced endocytosis. These findings indicate that ubiquitin-mediated degradation of the ZIP4 protein is critical for regulating zinc homeostasis in response to the upper tier of physiological zinc concentrations, via a process that is distinct from zinc-stimulated endocytosis.

Zinc is an essential trace element required for many enzymes as a catalytic cofactor and a critical component of structural motifs such as zinc fingers. However, zinc is also potentially toxic when allowed to accumulate beyond cellular needs. Thus, homeostatic mechanisms have evolved to precisely regulate intracellular levels of this nutrient. The importance of zinc in humans is illustrated by the genetic disorder of zinc deficiency acrodermatitis enteropathica (1–4). This disease is caused by mutations in ZIP4, a zinc importer required for the absorption of dietary zinc by enterocytes and in other cell types (2, 5, 6). Recent studies suggest that ZIP4 is regulated at multiple levels in response to changes in zinc availability. For example, in mice the levels of mZIP4 mRNA are increased in response to zinc limitation in enterocytes and yolk sac and suppressed upon zinc repletion (5, 7). Moreover, the abundance of mZIP4 protein at the plasma membrane of enterocytes is rapidly diminished when zinc-deficient mice are fed a zinc-replete diet (5), suggesting that the mZIP4 protein may be removed from the plasma membrane by zinc-stimulated endocytosis. Subsequent *in vitro* studies confirmed this in HEK293 cells transfected with recombinant mZIP4 protein (8). In these studies, human and murine ZIP4 was shown to accumulate at the plasma membrane during zinc deficiency and undergo endocytosis when cells were exposed to low zinc concentrations (~1 μM Zn). This Zn^{2+}-stimulated endocytosis of ZIP4 resulted in a reduction in ZIP4-dependent zinc uptake suggesting that this process controls the entry of zinc into cells (8).

In the current study, we demonstrate an additional level of regulation of ZIP4 involving ubiquitin-mediated degradation of the protein. ZIP4 protein was found to degrade at higher levels of zinc concentrations (10–20 μM) than those required to promote its endocytosis (~1 μM). Further analysis demonstrated that ZIP4 endocytosis was a prerequisite for ZIP4 degradation via a process that required both the proteasomal and lysosomal compartments. Overexpression of a dominant-negative ubiquitin mutant resulted in the suppression of Zn^{2+}-responsive ZIP4 degradation and co-immunoprecipitation experiments confirmed zinc-dependent ubiquitination of ZIP4. A histidine-rich putative zinc binding domain was required for zinc-induced degradation and ubiquitination. These findings identify Zn^{2+}-dependent ubiquitination and degradation of ZIP4 as an additional regulatory mechanism controlling zinc homeostasis.

EXPERIMENTAL PROCEDURES

Plasmids—The hZIP4 cDNA was cloned into the expression vector, pcDNA3.1, and the hemagglutinin (HA)[3] antigen epitope was added at the C terminus, as described previously (8). The hZIP4 mutations in this study were generated by PCR mutagenesis and subcloned into the pcDNA3.1 vector. N-terminal 3×FLAG-tagged human ubiquitin was kindly provided by Kazuo Sugamura and Nobuyuki Tanaka (Tohoku University, Japan). N-terminal 3×FLAG-tagged human ubiquitin K48R was generated using a QuikChange® II XL site-directed

* This work was supported by National Institutes of Health Grants DK66333 (to M. J. P.) and GM56285 (to D. E.). The costs of publication of this article were defrayed in part by the payment of page charges. This article must therefore be hereby marked "*advertisement*" in accordance with 18 U.S.C. Section 1734 solely to indicate this fact.

[1] Both authors contributed equally to this work.

[2] To whom correspondence should be addressed: Depts. of Biochemistry and Nutritional Sciences, 540d Life Sciences Center, University of Missouri-Columbia, Columbia, MO 65211. Tel.: 573-882-9685; Fax: 573-884-2537; E-mail: petrism@missouri.edu.

[3] The abbreviations used are: HA, hemagglutinin; HEK, human embryonic kidney; PBS, phosphate-buffered saline; TPEN, *N*,*N*,*N*′,*N*′-tetrakis(2-pyridylmethyl)ethylenediamine; GFP, green fluorescent protein.

mutagenesis kit (Stratagene). The GFP-tagged dynamin I-K44A mutant construct was kindly provided by Dr. Pietro DeCamilli (Yale University). The cytoplasmic loop (Leu^{424} to Met^{499}) containing the histidine-rich motif of wild-type hZIP4 or the 5H-5A mutant was subcloned into the pEGFP-N1 plasmid to assess sufficiency of this region for zinc-induced degradation.

Reagents, Cell Lines, and Antibodies—All chemicals, unless stated otherwise, were purchased from Sigma. The human embryonic kidney HEK293 cell line was maintained in Dulbecco's modified Eagle's medium containing 10% fetal bovine serum and 100 units/ml penicillin and streptomycin in a 5% CO_2, 37 °C incubator. HEK293 cells were transfected with the pcDNA3.1 empty vector or the same vector harboring the wild-type or mutant alleles of hZIP4 using the Lipofectamine 2000 reagent (Invitrogen) according to the manufacturer's instructions. Stably transfected cells were established by the selection with 500 μg/ml G418 in the growth medium (Amersham Biosciences). Transient transfections of plasmids expressing FLAG-tagged wild-type ubiquitin or ubiquitin-K48R, or GFP-tagged wild-type dynamin I or dynamin I-K44A were performed using the Lipofectamine 2000 reagent (Invitrogen). Cell viability assays were carried out using the Cell Proliferation Kit I (3-(4,5-dimethylthiazol-2-yl)-2,5-diphenyltetrazolium bromide, Roche Applied Science). All horseradish peroxidase-conjugated antibodies were from Roche Applied Science, and Alexa-488 and -588 conjugated antibodies were purchased from Invitrogen. All other antibodies were from Sigma. Zinc depletion of 10% fetal bovine serum-Dulbecco's modified Eagle's medium was performed using Chelex 100 as described previously (8).

Immunoblot Analysis—Cells cultured in 6-well trays were scraped into ice-cold phosphate-buffered saline (PBS) and pelleted by centrifugation. After several washes in ice-cold PBS, the cells were lysed by sonication in lysis buffer containing 62 mM Tris-Cl, pH 6.8, 2% SDS, 100 mM dithiothreitol, and protease inhibitor mix (Roche Applied Science). Samples were centrifuged for 10 min at 16,000 × *g*, and the protein concentration of the lysates was determined using a DC protein assay kit (Bio-Rad). 20 μg of protein lysates was separated using SDS-PAGE, transferred to nitrocellulose membranes, and detected by chemiluminescence (Pierce). As a loading control, the same membranes were stripped and re-probed with anti-tubulin antibody. In some experiments, cells were pretreated with 100 μg/ml cycloheximide added to the medium to inhibit protein synthesis prior to treatment with zinc or other metals. In other experiments, endocytosis inhibitors (sucrose or methyl-β-cyclodextrin) or proteasome inhibitors (MG132 or lactacystin) were added to culture medium as described in the text. Inhibition of glycosylation was performed using 1 μg/ml tunicamycin added to the medium for 24 h. Enzymatic removal of glycosyl groups was performed by addition of 2500 units of peptide *N*-glycosidase F (New England Biolabs) to cell lysates at 37 °C for 1 h.

Plasma Membrane Localization and Endocytosis Assays of hZIP4 Protein—The pool of hZIP4-HA at the plasma membrane was assessed by measuring the levels of anti-HA antibodies bound to the surface of HEK/hZIP4-HA cells as we have previously described for the murine ZIP4 protein (8). Briefly, HEK/hZIP4-HA cells in 6-well trays were washed twice with PBS on ice, blocked with ice cold 3% skim milk in PBS for 20 min, then incubated with 5 μg/ml anti-HA antibody for 1 h on ice. After extensive washing to remove unbound antibodies, cells were sonicated in SDS lysis buffer and lysates containing solubilized anti-HA antibodies were separated using SDS-PAGE and transferred to nitrocellulose membranes. Anti-HA antibodies were detected using horseradish peroxidase-conjugated antibodies (1:500) by chemiluminescence. The protein detected in the hZIP4-HA lane co-migrated with purified anti-HA antibody (data not shown).

Endocytosis of hZIP4-HA protein was indirectly determined by assaying the uptake of anti-HA antibodies added to the culture media of living cells as described previously (8). Cells were incubated at 37 °C in the indicated medium supplemented with 5 μg/ml anti-HA antibodies for 5 min to allow internalization of antibody/hZIP4-HA complexes by endocytosis. Cells were then transferred to ice to prevent further endocytosis then washed three times with ice-cold PBS, and surface-bound antibodies were removed by five washes with ice-cold acidic buffer (100 mM glycine, 20 mM magnesium acetate, 50 mM potassium chloride, pH 2.2). After two additional washes with ice-cold PBS, the cells were collected, lysed, and analyzed for anti-HA antibodies by immunoblotting as described above.

Immunofluorescence Microscopy—Cells were grown in 24-well trays for 24 h on sterile glass coverslips, washed twice with 1 ml of ice-cold PBS, and then fixed for 10 min at 25 °C using 4% paraformaldehyde. The cells were then permeabilized with 0.1% Triton X-100 in PBS for 5 min, blocked for 1 h with 1% bovine serum albumin and 3% skim milk in PBS, and then probed with the anti-HA antibodies (1:1000) followed by Alexa-488 anti-rabbit antibodies (1:1000).

^{65}Zn Uptake Assays—HEK293 cells transiently transfected with wild-type hZIP4-HA or the 5H-5A mutant were used for ^{65}Zn uptake assays as described previously (9). In brief, 48 h after transfection the cells were washed once in uptake buffer (15 mM HEPES, 100 mM glucose, and 150 mM KCl, pH 7.0) and then incubated with uptake buffer containing the indicated concentrations of $^{65}ZnCl_2$ (PerkinElmer Life Sciences) at 37 °C for 10 min. Assays were stopped by adding an equal volume of ice-cold uptake buffer supplemented with 1 mM EDTA (stop buffer). Cells were then collected on nitrocellulose filters (Millipore, 0.45-μm pore size) and washed three times in stop buffer. Cell-associated radioactivity was measured with a Packard Auto-Gamma 5650 gamma counter. Duplicate samples were assayed for protein determination using the Bio-Rad DC protein assay and used to calculate zinc uptake rate.

Immunoprecipitation Experiments—hZIP4-HA-expressing HEK293 cells or vector controls were transiently transfected with 10 μg of the 3×FLAG-Ubiquitin construct and then incubated for the indicated times in zinc-depleted or zinc-supplemented medium. Cells were scraped into ice-cold PBS and pelleted by centrifugation and then lysed in radioimmune precipitation assay buffer (150 mM NaCl, 1% Nonidet P-40, 0.5% sodium deoxycholate, 0.1% SDS, 50 mM Tris-HCl, pH 8.0, and protease inhibitor mix (Roche Applied Science)) for 30 min at 4 °C with rotation. Samples were centrifuged for 10 min at

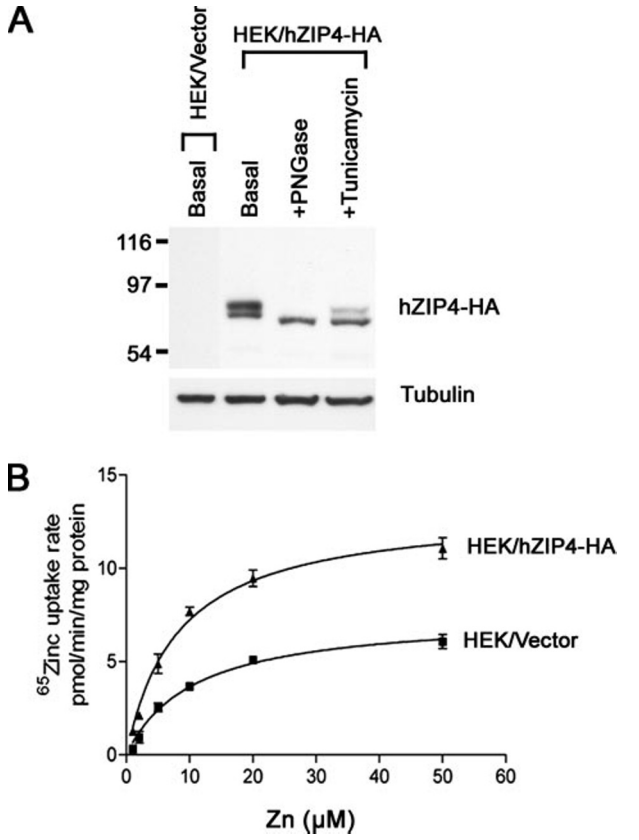

FIGURE 1. **Characterization of the hZIP4-HA protein in HEK293 cells.** *A*, immunoblot detection of the hZIP4-HA protein in HEK/hZIP4-HA cells using anti-HA antibodies revealed a specific doublet band of 80 kDa and 85 kDa that was not observed in vector-transfected control cells. Removal of glycosylation moieties by treatment of cell lysates with peptide *N*-glycosidase F shifted the hZIP4-HA doublet to a single band (*lane 3*). Exposure of HEK/hZIP4-HA cells to tunicamycin for 14 h to prevent glycosylation also enriched the abundance of this smaller hZIP4-HA protein (*lane 4*), suggesting that both hZIP4-HA bands are likely different glycosylated species. *B*, hZIP4-HA is a functional zinc transporter. ^{65}Zn accumulation by HEK/hZIP4-HA and HEK/vector cells was assayed in buffer containing indicated concentrations of zinc. Zinc uptake rate was normalized to protein concentration. Each point represents the mean of three representative experiments, and the *error bars* indicate ± 1 S.D.

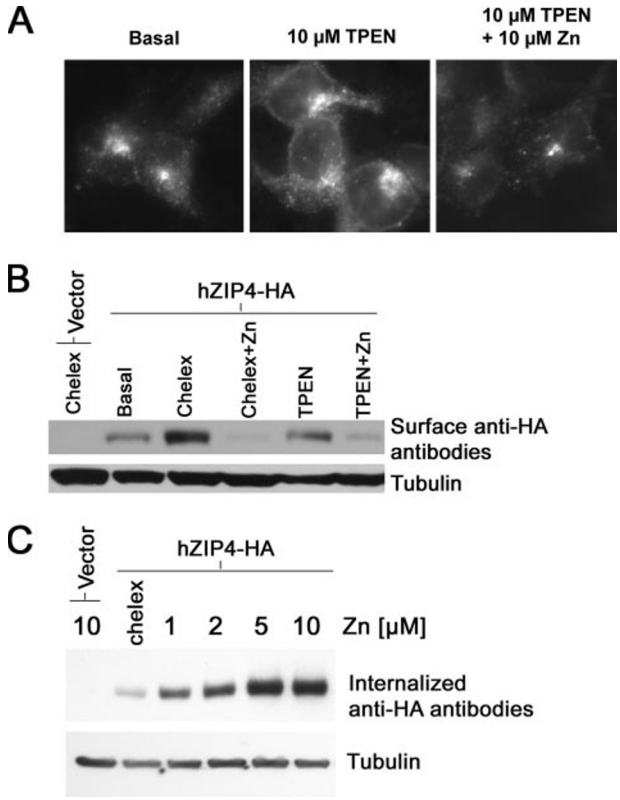

FIGURE 2. **The plasma membrane abundance and endocytosis of the hZIP4-HA protein is regulated by zinc availability.** *A*, immunofluorescence microscopy detection of hZIP4-HA in HEK/hZIP4-HA cells exposed for 1 h to basal medium, basal medium plus 10 μM TPEN, or basal medium plus 10 μM TPEN and 10 μM Zn^{2+}. *B*, zinc availability alters plasma membrane levels of hZIP4-HA in HEK/hZIP4-HA cells. Cells were cultured for 1 h in basal medium, Chelex-treated medium, Chelex-treated medium plus 10 μM Zn^{2+}, basal medium plus 10 μM TPEN, or basal medium plus 10 μM TPEN and 10 μM Zn^{2+}. Cells were then fixed, and the surface pool of hZIP4-HA protein was probed with anti-HA antibody. Antibodies retained by cells were detected by immunoblot using horseradish peroxidase-conjugated secondary antibodies. *C*, zinc stimulates the endocytosis of hZIP4-HA protein. HEK/hZIP4-HA cells were preincubated with Chelex-treated medium for 1 h to maximize surface levels of hZIP4-HA, before supplemented with the indicated zinc concentrations and anti-HA antibodies were added to these media before allowing endocytosis to proceed for 5 min. Surface-bound antibodies were removed from cells by acidic buffer washes and internalized anti-HA antibodies were detected by immunoblotting.

16,000 × *g*, and the protein concentration of the lysates was determined using the DC protein assay kit (Bio-Rad). The cell lysates were pre-cleared with Protein-G-agarose (Roche Applied Science) overnight at 4 °C with rotation, followed by incubation with anti-HA affinity matrix (Roche Applied Science) for 4 h at 4 °C with rotation. The anti-HA affinity matrix was washed three times with radioimmune precipitation assay lysis buffer before the proteins were eluted by boiling at 95 °C for 5 min in elution buffer. The eluates were run on 4–20% SDS-PAGE gradient gels, transferred to nitrocellulose membranes, and the extent of hZIP4-HA ubiquitination was assessed by probing with anti-FLAG M2 monoclonal antibody-horseradish peroxidase conjugate (1:1,000) by chemiluminescence (Pierce). Duplicate samples were probed by anti-HA antibody (1:2,000) followed by horseradish peroxidase-conjugated secondary antibodies (1:5,000). Meanwhile, total cell lysates were run on SDS-PAGE gel and probed by either anti-HA antibody (1:2,000) or by anti-tubulin antibody (1:10,000) followed by horseradish peroxidase-conjugated secondary antibodies.

RESULTS

hZIP4-HA Is a Glycosylated Protein and Functional Zinc Transporter That Undergoes Zinc-responsive Endocytosis—Recent studies have demonstrated that the murine ZIP4 protein is a high affinity zinc importer and undergoes zinc-stimulated endocytosis in response to low micromolar zinc concentrations (5, 8–11). We began this study by determining if the human ZIP4 protein also exhibits these properties in transfected HEK293 cells. An HA antigen tag was fused to the extracellular C terminus of hZIP4, and stably transfected HEK293 cells expressing the hZIP4-HA protein were isolated (HEK/hZIP4-HA cells). Western blot analysis using anti-HA antibodies indicated that the hZIP4-HA protein was resolved at an apparent molecular mass of ~85 kDa, as well as a faster migrating protein of 80 kDa (Fig. 1*A*). Both bands were absent in HEK293 cells transfected with vector alone indicating they were specific for the hZIP4-HA protein. The presence of two hZIP4-HA bands was likely due to variation in glycosylation,

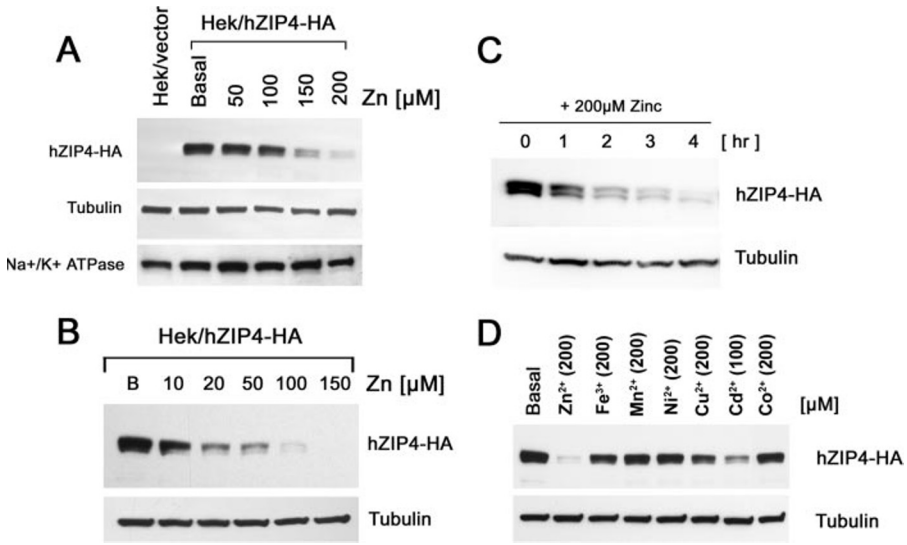

FIGURE 3. **Elevated zinc concentrations reduce levels of hZIP4-HA protein.** *A*, immunoblot analysis of total hZIP4-HA protein in HEK/hZIP4-HA cells after exposure to elevated zinc concentrations. HEK293 cells stably expressing the pcDNA3.1 vector or hZIP4-HA were pretreated for 30 min with cycloheximide (100 μg/ml) to inhibit new protein synthesis followed by a 4-h exposure to the indicated concentrations of zinc. Protein lysates were separated by SDS-PAGE, and hZIP4-HA protein was detected using anti-HA antibodies. Tubulin was detected as the loading control. *B*, dose-dependent degradation of hZIP4-HA by zinc. Immunoblots were used to detect the abundance of hZIP4-HA protein in HEK/hZIP4-HA cells treated with the indicated concentrations of zinc for 18 h. *C*, time-dependent degradation of the hZIP4-HA protein by zinc. HEK/hZIP4-HA cells were pretreated for 30 min with cycloheximide (100 μg/ml) to inhibit new protein synthesis followed by zinc treatment for indicated times. Immunoblots were used to detect hZIP4-HA protein as described in A above. *D*, metal specificity of the hZIP4-HA degradation response. HEK/hZIP4-HA cells were pretreated with cycloheximide followed by exposure to either basal medium or basal media containing indicated concentrations of trace metals for 4 h. Total cell lysates were immunoblotted with anti-HA antibodies to detect hZIP4-HA protein.

because removal of carbohydrate moieties using peptide *N*-glycosidase F, or prevention of glycosylation *in vivo* using tunicamycin, resulted in a predominant band of 70 kDa, which is the expected molecular mass of hZIP4-HA (Fig. 1*A*). Kinetic studies using ^{65}Zn demonstrated that the hZIP4-HA protein was a functional zinc transporter, as evident from the 2-fold increase in total zinc accumulation in HEK/hZIP4-HA cells compared with HEK/vector cells over a range of zinc concentrations (Fig. 1*B*). The apparent K_m for hZIP4-HA-dependent zinc uptake was 2.5 μM, which was similar to the reported value for murine ZIP4 and other mammalian ZIP family members (5, 9, 10, 12, 13).

Immunofluorescence microscopy revealed that the hZIP4-HA protein was localized within cytoplasmic vesicles that were concentrated in the perinuclear region when HEK/hZIP4-HA cells were cultured in basal media (Fig. 2*A*). However, depletion of zinc in the medium using the zinc chelator TPEN resulted in the dispersal of hZIP4-HA to the cell periphery, consistent with an increased abundance at the plasma membrane. The extracellular orientation of the HA-epitope tag fused to the C terminus of hZIP4 allowed levels of hZIP4-HA to be determined at the plasma membrane of intact cells by immunoblot analysis of anti-HA antibodies recovered from HEK/hZIP4-HA cells. Using this approach, we observed an increase in hZIP4-HA protein levels at the plasma membrane of HEK/hZIP4-HA cells under zinc limiting conditions relative to basal medium (Fig. 2*B*). This increase in hZIP4-HA protein at the plasma membrane during zinc limitation was likely due to a decrease in its endocytosis, as we have found previously for the mZIP4-HA protein (8). Once again the extracellular orientation of the HA-tag on the C terminus of hZIP4-HA enabled hZIP4-HA endocytosis to be indirectly measured by the internalization of anti-HA antibody added to the culture media of living cells, as we have done previously for mZIP4-HA (8). A low level of anti-HA antibody uptake was observed for HEK/hZIP4-HA cells in media made zinc-deficient using Chelex 100 (Fig. 2*C*). However, when zinc was added to Chelex-treated media there was a concentration-dependent increase in hZIP4-HA endocytosis, as determined by the marked increase in anti-HA antibody uptake during a 5-min incubation. As expected the HEK/vector cells, which lack hZIP4-HA, failed to internalize anti-HA antibodies. Taken together, these data suggest that plasma membrane abundance of hZIP4-HA is dependent on zinc status and that hZIP4-HA undergoes zinc-induced endocytosis.

hZIP4-HA Is Degraded by Elevated Zinc—There are many examples of proteins that are degraded upon endocytosis from the plasma membrane (14–16). To explore whether such regulation occurs for hZIP4, we examined the steady-state levels of this protein in zinc-treated cells. HEK/hZIP4-HA cells were pre-treated with 100 μg/ml cycloheximide to inhibit new protein synthesis, and then the level of hZIP4-HA protein was determined after exposing cells to different zinc concentrations for 4 h. Significantly, this zinc treatment resulted in dose-dependent decrease in levels of hZIP4-HA protein (Fig. 3*A*), which was most apparent at between 150 and 200 μM zinc. This zinc treatment had no effect on the steady-state levels of another membrane transporter, Na^+/K^+ ATPase (Fig. 3*A*), suggesting that this degradation response specifically affects hZIP4-HA. Zinc-stimulated degradation of hZIP4-HA occurred as rapidly as 1 h following addition of 200 μM zinc (Fig. 3*C*), and as little as 10–20 μM zinc could stimulate the degradation of hZIP4-HA with longer exposures (18 h) (Fig. 3*B*). The metal specificity of the hZIP4-HA degradation response was examined by exposing HEK/hZIP4-HA cells to various metals at 200 μM (100 μM for cadmium) for 4 h. Besides zinc, cadmium was the only metal tested that promoted hZIP4-HA degradation (Fig. 3*D*).

To further characterize the zinc-stimulated degradation of hZIP4-HA, we determined whether this process required endocytosis. Endocytosis was blocked using the dominant-negative dynamin mutant (Dyn1-K44A), which is required for the pinching of endocytic vesicles at the plasma membrane (17). In HEK/hZIP4-HA cells transiently transfected with a GFP-tagged Dyn1-K44A construct, the hZIP4-HA protein accumulated at the plasma membrane, as shown by immunofluorescence microscopy (Fig. 4*A*) and cell surface labeling of cells with

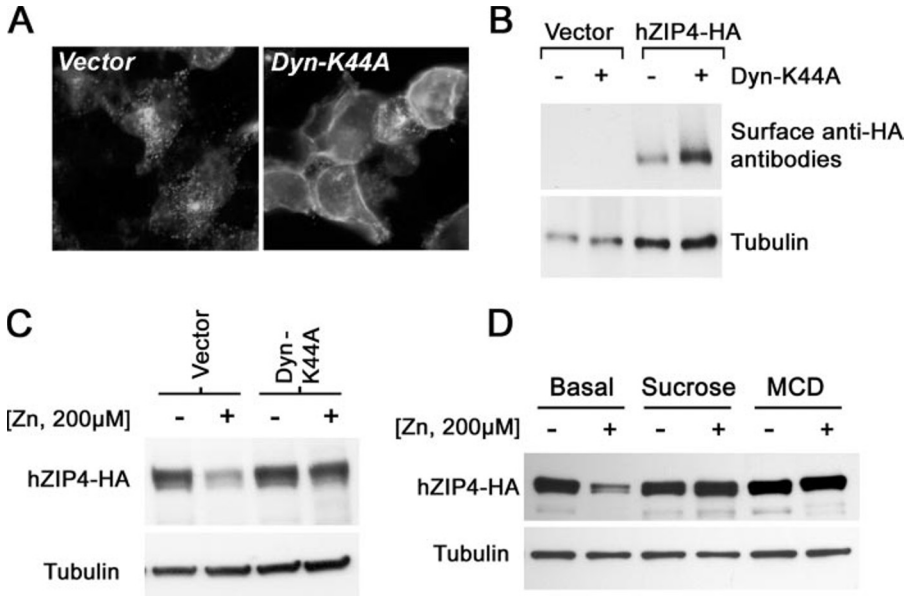

FIGURE 4. **Endocytosis inhibitors block zinc-induced hZIP4-HA degradation.** *A*, immunofluorescence analysis of hZIP4-HA protein in HEK/hZIP4-HA cells transiently transfected with a plasmid expressing the dynamin-K44A mutant or control vector. Cells were fixed at 16 h post-transfection and probed with rabbit anti-HA antibody, followed by Alexa 488-conjugated secondary antibody. *B*, immunoblot analysis of plasma membrane levels of hZIP4-HA in HEK/vector or HEK/hZIP4-HA cells transiently transfected with the dynamin-K44A mutant or control vector. Surface hZIP4-HA protein levels were determined by immunoblot analysis of the anti-HA antibodies bound to surface of non-permeabilized cells as described in the Fig. 2 legend. *C*, effect of dynamin-K44A expression on zinc-stimulated degradation of hZIP4-HA. HEK/hZIP4-HA cells were transiently transfected with either empty vector or the dynamin-K44A expression plasmid. Cells were then pretreated for 30 min with cycloheximide to inhibit protein synthesis followed by a 4-h exposure to either basal medium or basal medium containing 200 μM Zn. hZIP4-HA protein was then detected in total lysates by immunoblotting. *D*, other endocytosis inhibitors block zinc-stimulated degradation of hZIP4-HA. HEK/hZIP4-HA cells were pretreated with cycloheximide and the endocytosis inhibitors sucrose or methyl-β-cyclodextrin. Cells were then exposed for 4 h in basal medium or basal medium containing 200 μM zinc. Total protein extracts were separated by SDS-PAGE and transferred to nitrocellulose membranes, and hZIP4-HA proteins were detected using immunoblotting.

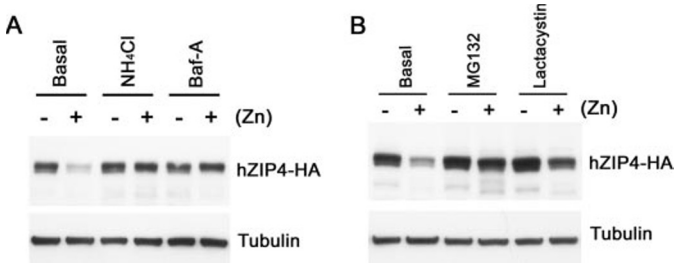

FIGURE 5. **hZIP4-HA degradation requires both proteasomal and lysosomal degradation pathways.** Proteasome and lysosome inhibitors block zinc-dependent degradation of hZIP4-HA. HEK/hZIP4-HA cells were pretreated for 30 min with cycloheximide and the lysosome inhibitors NH_4Cl or bafilomycin (*A*) or the proteasome inhibitors, MG132 or lactacystin (*B*). Cells were then exposed for an additional 4 h in basal medium or basal medium containing 200 μM zinc in the continued presence of the above inhibitors. Total protein lysates from cells were separated by SDS-PAGE, and hZIP4-HA protein abundance was determined by immunoblotting with the anti-HA antibody.

anti-HA antibodies (Fig. 4*B*). We then examined the effect of Dyn1 K44A-mediated inhibition of endocytosis on zinc-stimulated degradation of hZIP4-HA. As shown in Fig. 4*C*, the Dyn1-K44A mutant suppressed the degradation of hZIP4-HA in response to elevated zinc concentrations. Moreover, pharmacological inhibition of endocytosis using methyl-β-cyclodextrin or sucrose also impaired the degradation of hZIP4-HA in zinc-treated HEK/hZIP4-HA cells (Fig. 4*D*). These findings suggested that the degradation of hZIP4-HA in response to elevated zinc concentrations requires endocytosis of the protein.

To further characterize the mechanism underlying the zinc-stimulated degradation of hZIP4, we examined the effects of lysosome and proteasome inhibitors on this process. The lysosome inhibitors, ammonium chloride and bafilomycin, and the proteasome inhibitors, MG132 and lactacystin, blocked the zinc-stimulated degradation of hZIP4-HA (Fig. 5, *A* and *B*). Control experiments indicated that none of these inhibitors blocked endocytosis of the hZIP4-HA protein (data not shown). These findings suggest that the degradation of hZIP4-HA requires both lysosomal and proteasomal pathways.

Polyubiquitin-mediated hZIP4-HA Degradation—Because proteasome degradation is usually preceded by polyubiquitination of the target protein, we investigated whether hZIP4-HA was ubiquitinated by zinc treatment. Protein degradation via proteasome degradation pathways usually involves polyubiquitination of lysine 48 of the ubiquitin molecule (18, 19). Therefore, we made a dominant-negative ubiquitin mutant in which lysine 48 was mutated to arginine (ubiquitin-K48R). As shown in Fig. 6 (*A* and *B*), HEK/hZIP4-HA cells transiently transfected with ubiquitin-K48R impaired the degradation of the hZIP4-HA protein in zinc-treated cells in contrast to mock transfected cells. These findings suggest that polyubiquitination is involved in zinc-regulated hZIP4 degradation.

To further verify the role of ubiquitin in zinc-stimulated degradation of hZIP4, we tested whether ubiquitin could be co-precipitated with hZIP4 in zinc-treated cells. HEK/hZIP4-HA cells were transiently transfected with a FLAG-ubiquitin construct and incubated overnight in basal medium followed by a 4-h incubation in medium made zinc-deficient by Chelex treatment or basal medium supplemented with 200 μM zinc in the presence of MG132 to block hZIP4-HA degradation. Anti-HA antibodies were used to immunoprecipitate hZIP4-HA from cell lysates, which were then immunoblotted for ubiquitin using anti-FLAG antibodies. In precipitates from zinc-treated HEK/hZIP4-HA cells, anti-FLAG antibodies against ubiquitin detected an intense band at 100 kDa as well as a series of larger bands consistent with polyubiquitinated hZIP4 species (Fig. 6*C*). These ubiquitinated forms of hZIP4-HA were markedly reduced in HEK/hZIP4-HA grown under zinc-deficient conditions and absent in vector-transfected control cells. Taken together with earlier data, these findings suggest that zinc-stimulated degradation of the hZIP4 protein involves polyubiquitination.

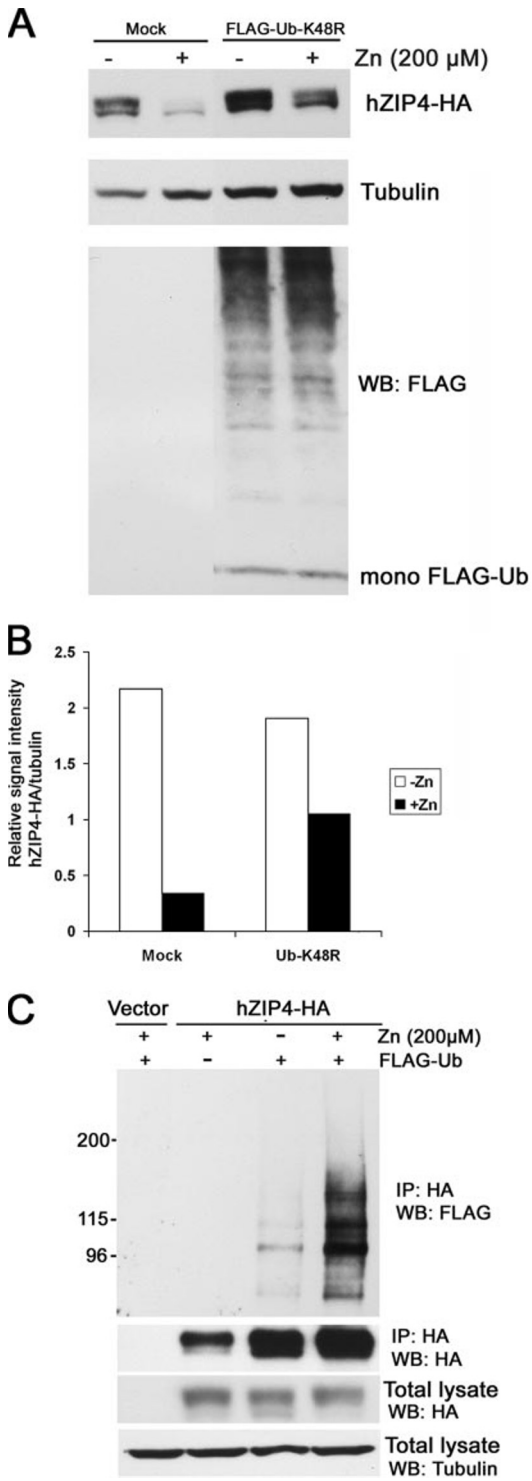

FIGURE 6. **Zinc-stimulated degradation of hZIP4-HA involves polyubiquitination.** *A*, immunoblot detection of hZIP4-HA protein in mock transfected or ubiquitin-K48R-transfected HEK293/hZIP4-HA cells exposed to basal or elevated zinc concentrations. At 24 h post-transfection, cells were pretreated with cycloheximide to inhibit protein synthesis prior to a 4-h exposure to basal medium or basal medium supplemented with 200 μM zinc. Total protein extracts were separated by SDS-PAGE and transferred to nitrocellulose membranes, and hZIP4-HA protein was detected using anti-HA antibodies. Ubiquitin-K48R was detected using anti-FLAG antibodies. *B*, relative signal intensity of hZIP4-HA normalized to tubulin is shown from immunoblot in *A*. *C*, HEK/hZIP4-HA cells or HEK293 cells transfected with pcDNA3.1 vector were transiently transfected with the FLAG-ubiquitin plasmid. Following a 24-h recovery, cells were pretreated for 30 min with cycloheximide to inhibit protein synthesis, and MG132 to inhibit proteasomal degradation, while exposed to zinc-deficient Chelex-treated medium, or prior to exposure to basal medium supplemented with 200 μM zinc, for 4 h. Cell lysates were passed over anti-HA affinity matrix (*IP:HA*), and the retained fraction was run on 4–20% SDS-PAGE gradient gels and then transferred to nitrocellulose membranes. Western blotting was used to determine the extent of ubiquitination (*IP:HA* and *WB:FLAG*) in comparison to immunoprecipitated hZIP4-HA protein (*IP:HA* and *WB:HA*). Total cell lysates from the same samples were used to detect hZIP4-HA protein and tubulin.

A Conserved Histidine-rich Motif Is Required for Zinc-stimulated hZIP4-HA Degradation—A characteristic feature of several ZIP family members is a cluster of histidine residues in a cytoplasmic loop connecting transmembrane domains 3 and 4 (20–25). This sequence is highly reminiscent of several zinc binding centers, particularly hydrolases, which possess a conserved sequence HE*XX*H*XX*G*XX*H or HX_nH (where $n < 5$) (26). The histidine-rich motif in hZIP4 is ^{438}HSSHSHGGHSH^{448} (Fig. 7*A*), and this motif may be required for zinc-dependent ubiquitination and degradation of the protein by functioning as a zinc sensor. To test this hypothesis, we investigated the effect on hZIP4 degradation of a deletion mutant encompassing the region Cys^{436} to His^{448} (Fig. 7*A*). Significantly, this mutation completely abolished zinc-stimulated hZIP4 degradation, suggesting that this histidine-rich cluster was essential for this process (Fig. 7*B*). To further characterize this histidine-rich cluster, we replaced individual histidines with alanine and tested the effect on zinc-dependent degradation in stably transfected HEK cells (Fig. 7*A*). None of the individual histidine mutations abolished zinc-dependent degradation suggesting that no single histidine residue was solely responsible for this response (Fig. 7*C*). Moreover, alanine substitution of the first two histidines (2H-2A) or the last three histidines (3H-3A) failed to abolish zinc-stimulated degradation of hZIP4 (Fig. 7*D*). However, mutation of all five histidine residues to alanine (5H-5A) within this cluster completely abolished zinc-dependent degradation of hZIP4 (Fig. 7*E*). These findings suggest that individual histidines within this cluster are dispensable for hZIP4 degradation; however, loss of all five histidines abolishes this response. Cadmium-dependent degradation was also inhibited by this mutation suggesting that both zinc and cadmium degrade hZIP4 via a common mechanism involving this motif.

Because zinc-dependent degradation of hZIP4 required the histidine-rich cluster, we hypothesized that this motif may also be essential for zinc-dependent ubiquitination. This hypothesis was supported by the finding that zinc failed to stimulate the ubiquitination of the hZIP4–5H-5A protein (Fig. 8*A*). Control immunoblots using anti-HA antibodies indicated that levels of immunoprecipitated hZIP4 protein were similar for wild-type and mutant protein (Fig. 8*A*). This impairment of zinc-stimulated degradation of the hZIP4–5H-5A protein was not due to a defect in zinc-stimulated endocytosis as shown in Fig. 8*B*. Collectively, these findings suggest that the cytoplasmic histidine-rich cluster is essential for zinc-stimulated ubiquitination and degradation of hZIP4.

We reasoned that, if the degradation of hZIP4 by zinc serves to protect against zinc toxicity, the failure of this response for the hZIP4–5H-5A protein may confer hypersensitivity to zinc. To test this hypothesis, we assayed the viability of HEK/hZIP4-

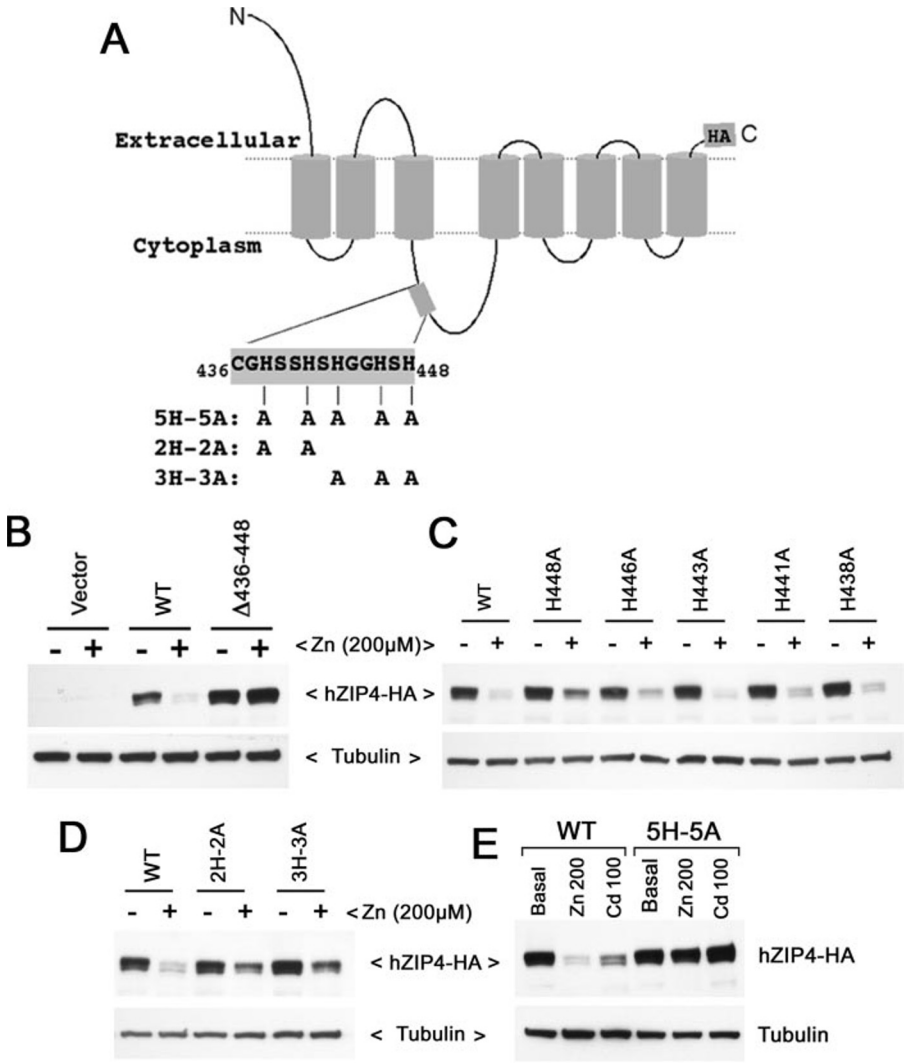

FIGURE 7. **Zinc-stimulated hZIP4-HA degradation requires a cytoplasmic histidine-rich sequence.** *A*, schematic illustration of the hZIP4-HA protein with highlighted histidine-rich sequence in the second cytoplasmic loop. Mutations introduced within this sequence are shown. *B–E*, immunoblot analysis of zinc-stimulated degradation of hZIP4-HA mutations in the histidine-rich cluster. Stable transfectants of each mutation in *A* were exposed to basal or zinc supplemented media for 4 h (or cadmium, *E*), and the levels of each mutant protein were determined by anti-HA immunoblot.

HA, HEK/hZIP4–5H-5A, and HEK/vector cells exposed to a range of zinc concentrations. As shown in Fig. 8*C*, cells expressing the hZIP4-HA wild-type protein were more sensitive to zinc than those harboring the empty vector. However, cells expressing the hZIP4–5H-5A mutant protein were hypersensitive to zinc compared with cells expressing wild-type hZIP4-HA or vector-only cells. Zinc uptake studies confirmed that the 5H-5A mutant was a functional transporter, although it exhibited a 2-fold reduction in V_{max} relative to wild type, whereas its K_m was unaffected (Fig. 8*D*). Taken together, these data suggest that the histidine-rich cluster is essential for zinc-stimulated ubiquitination and degradation of hZIP4, which is a regulatory mechanism that protects against zinc overload.

The histidine-rich motif in the cytoplasmic loop between transmembrane domains 3 and 4 was further characterized by determining if it is sufficient for zinc-induced degradation activity. A fusion protein was generated between the cytoplasmic loop of hZIP4 and the N terminus of GFP (Wt-loop-GFP) or the 5H-5A mutation and GFP (5H-5A-loop-GFP). HEK293 cells were stably transfected with either GFP vector alone, or plasmids harboring Wt-loop-GFP or 5H-5A-loop-GFP. Treatment of these cells with elevated zinc concentrations failed to stimulate degradation of either the Wt-loop-GFP or the 5H-5A-loop-GFP protein (Fig. 9). These findings suggest that the histidine-rich domain is essential but not autonomously sufficient for hZIP4 degradation.

DISCUSSION

The ZIP4 protein is regulated at multiple levels in response to changing zinc concentrations. Studies in mice have shown that the levels of mZIP4 mRNA in enterocytes and visceral yolk sac respond to changes in dietary zinc availability. Moreover, the abundance of the mZIP4 protein at the plasma membrane of these tissues is similarly regulated. Studies using ZIP4-transfected cells have shown that the mouse and human ZIP4 proteins cycle between cytoplasmic vesicles and the plasma membrane and that the endocytic arm of this cycling pathway is stimulated by low micromolar concentrations of zinc (Fig. 2*C*) (8). Each of these homeostatic processes function to maximize the ZIP4-dependent zinc uptake at the plasma membrane during zinc limitation and to down-regulate this function during zinc repletion. In this study we identify an additional level of regulation at the upper tier of physiological zinc concentrations (>20 μM zinc) involving degradation of the protein.

The zinc-stimulated degradation of hZIP4 was dependent on its endocytosis from the plasma membrane, and, consistent with this observation, the degradation was blocked by inhibitors of lysosomal acidification. Interestingly, hZIP4 degradation was also impaired by inhibitors of the 26 S proteasome, as well as by a dominant-negative ubiquitin mutant that inhibits polyubiquitination. These findings suggest that the degradation of hZIP4 requires both the ubiquitin-26 S proteasome pathway as well as the lysosomal pathway. However, we recognize that the role of the proteasome is not definitive, because inhibition of proteasome function may indirectly prevent hZIP4 degradation by depleting recycled ubiquitin substrate for mono-ubiquitination of the protein. Nevertheless, our findings are reminiscent of several other proteins whose proteolysis requires both the proteasome

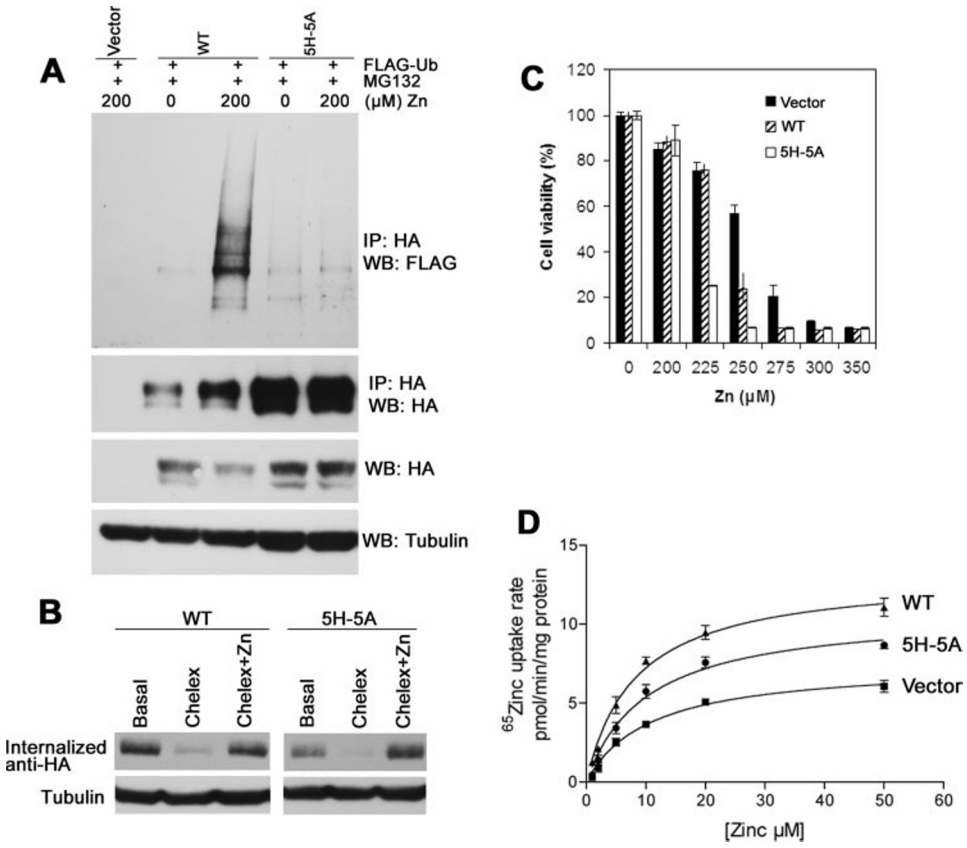

FIGURE 8. **Zinc-stimulated hZIP4-HA ubiquitination requires the cytoplasmic histidine-rich sequence.** *A*, HEK293 cells stably expressing pcDNA3.1 vector, hZIP4-HA wild-type, or hZIP4–5H-5A were transiently transfected with the FLAG-ubiquitin plasmid. Cells were pretreated with cycloheximide and MG132 (to block new protein synthesis and hZIP4 degradation) for 30 min while exposed to Chelex-treated medium, or prior to exposure to basal medium supplemented with 200 μM zinc, for 4 h. Cell lysates were passed over anti-HA affinity matrix (*IP:HA*), and the retained fraction was run on 4–20% SDS-PAGE gradient gels. Western blotting was used to determine the extent of ubiquitination (*IP:HA* and *WB:FLAG*) in comparison to immunoprecipitated hZIP4-HA protein (*IP:HA* and *WB:HA*). Total cell lysates from the same samples were used to detect total abundance of hZIP4-HA protein and tubulin. *B*, zinc-stimulated hZIP4–5H-5A endocytosis. HEK/hZIP4-HA wild-type or HEK/hZIP4–5H-5A cells were preincubated in Chelex-treated medium for 1 h to maximize surface levels of hZIP4-HA. Endocytosis of anti-HA antibodies was then examined in basal medium, Chelex-treated medium, or Chelex-treated medium plus 10 μM zinc. Internalized anti-HA antibodies were detected by immunoblotting. *C*, HEK/vector, HEK/hZIP4-HA wild-type, or HEK/hZIP4–5H-5A cells were grown for 2 days in basal medium supplemented with the indicated concentrations of zinc. Cells were then assayed for viability by 3-(4,5-dimethylthiazol-2-yl)-2,5-diphenyltetrazolium bromide assay. Each value represents the mean of a representative experiment ($n = 3$) ± S.D. *D*, analysis of zinc uptake by the hZIP4-HA-5H-5A protein. ^{65}Zn accumulation by HEK/vector, HEK/hZIP4-HA wild-type, or HEK/hZIP4–5H-5A cells in buffer containing indicated concentrations of zinc are shown. The zinc uptake rate was normalized to protein concentration. *Error bars* indicate ±1 S.D.

and lysosome (27–30). The process by which the proteasome and lysosome are involved in protein degradation is not fully understood. However, recent studies have shown that the proteasome is involved in the targeting of some membrane proteins from late endosomes to lysosomes (27, 29, 30). Whether such a role exists for hZIP4 is yet to be determined.

Our studies have identified the histidine-rich cluster in the cytoplasmic domain of hZIP4 as a critical determinant of zinc-stimulated ubiquitination and degradation. Although the role of this sequence as a zinc ligand has not been confirmed, the demonstration of a zinc-dependent function for this sequence is consistent with a role in zinc binding. This histidine-rich cluster may function as a sensor of cytoplasmic zinc concentration that promotes hZIP4 ubiquitination when zinc reaches a critical threshold, possibly via a conformational change that exposes a lysine residue in the cytoplasmic portions of the protein. Lysine 463 is a likely candidate, because this residue is conserved in mammalian ZIP4 homologues. These findings are reminiscent of the yeast *Saccharomyces cerevisiae* high affinity zinc transporter ZRT1, which undergoes ubiquitin-dependent degradation in the vacuole (31, 32). Our studies demonstrated that mutation of all five histidines of the histidine cluster was required to abolish zinc-stimulated degradation of hZIP4, suggesting that there may be redundancy in their zinc binding function. Moreover, the cytoplasmic loop containing this histidine-rich sequence probably functions as a degradation motif only in the context of the complete hZIP4 protein, because fusion of this region to an unrelated protein, GFP, failed to confer zinc-dependent regulation of the chimeric protein.

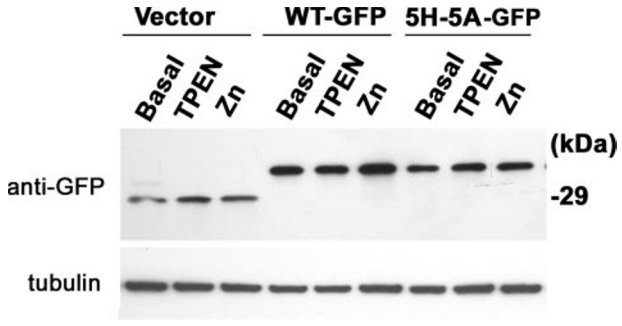

FIGURE 9. **Analysis of zinc-stimulated degradation of a chimeric fusion between the hZIP4 histidine-rich cytoplasmic loop (Leu^{424} to Met^{499}) and GFP.** Western blot analysis of Wt-loop-GFP and 5H-5A-loop-GFP protein levels under varying zinc concentrations. Cells were cultured for 4 h in basal medium, basal medium plus 10 μM TPEN, or basal medium plus 200 μM zinc. Anti-GFP antibodies were used to detect levels of chimeric fusion proteins.

Another notable finding was that the 5H-5A mutation did not affect zinc-stimulated endocytosis of hZIP4, suggesting that degradation and endocytosis are regulated by different zinc-sensing mechanisms. Consistent with this postulate was the finding that hZIP4 endocytosis was responsive to sub-micromolar zinc concentrations, whereas the degradation required zinc concentrations an order of magnitude greater (>20 μM). Interestingly, this is similar to zinc concentrations required to induce the expression of metallothioneins via the metal response element-binding transcription factor 1 (MTF-1) (33, 34). Metallothioneins are cysteine-rich cytoplas-

mic proteins that bind excess zinc and protect against zinc overload. Our finding that the 5H-5A mutant protein rendered cells more sensitive to elevated zinc concentrations relative to wild-type hZIP4 suggests that the degradation response controlled by this histidine-rich cluster is an additional mechanism to protect cells against zinc toxicity. Interestingly, cadmium was also found to induce degradation of hZIP4 via a process that was dependent on the histidine-rich motif. This property of cadmium is likely a reflection of its ability to mimic zinc binding to histidine residues. It will be of interest to test whether this mechanism is protective against cadmium toxicity, as was the case for zinc.

A key question to be addressed is why multiple levels of ZIP4 regulation exist. Mammalian ZIP4 is expressed at highest levels in intestinal enterocytes where responses to a wide range of zinc concentrations from dietary sources are likely to be important for zinc uptake and prevention of zinc toxicity. The regulation of ZIP4 mRNA levels by zinc would provide a set point of ZIP4 expression, which responds slowly to changes in dietary zinc content relative to endocytosis (hours *versus* minutes). Interestingly, this regulation of intestinal mZIP4 mRNA also responds to body zinc status, because intestinal mZIP4 mRNA levels are regulated by systemic zinc concentrations (5, 6, 33). Thus, regulation of mZIP4 mRNA may provide a set point of mZIP4 expression, after which the post-translational regulatory mechanisms, endocytosis and degradation, further regulate zinc accumulation. Our studies demonstrate that zinc-stimulated endocytosis of ZIP4 protein occurs within minutes and responds to low micromolar levels of zinc (8, 10, 11). The rapidity of this response, and its dependence on extracellular zinc-binding residues,[4] suggests that endocytosis may be regulated by dietary zinc concentrations rather than systemic or cytoplasmic zinc content. The down-regulation of ZIP4 protein levels has been shown to occur in mice exposed to elevated zinc concentrations (5, 7, 35), and our findings in cultured cells suggest that the proteasomal/lysosomal system may be responsible for this regulation. It will be of interest to determine whether the ubiquitin-dependent degradation of ZIP4 in the intestine is responsive to an overload of dietary zinc concentrations or systemic zinc status, and whether this process functions to protect against zinc toxicity in the enterocyte or at the organismal level.

Acknowledgments—We are indebted to Michelle Mooney for her excellent technical assistance. We also thank Zhongji Liao for his helpful discussion on immunoprecipitation experiments.

REFERENCES

1. Kury, S., Kharfi, M., Kamoun, R., Taieb, A., Mallet, E., Baudon, J. J., Glastre, C., Michel, B., Sebag, F., Brooks, D., Schuster, V., Scoul, C., Dreno, B., Bezieau, S., and Moisan, J. P. (2003) *Hum. Mutat.* **22,** 337–338
2. Wang, K., Zhou, B., Kuo, Y. M., Zemansky, J., and Gitschier, J. (2002) *Am. J. Hum. Genet.* **71,** 66–73
3. Kury, S., Dreno, B., Bezieau, S., Giraudet, S., Kharfi, M., Kamoun, R., and Moisan, J. P. (2002) *Nat. Genet.* **31,** 239–240
4. Nakano, A., Nakano, H., Nomura, K., Toyomaki, Y., and Hanada, K. (2003) *J. Invest. Dermatol.* **120,** 963–966
5. Dufner-Beattie, J., Wang, F., Kuo, Y. M., Gitschier, J., Eide, D., and Andrews, G. K. (2003) *J. Biol. Chem.* **278,** 33474–33481
6. Liuzzi, J. P., Bobo, J. A., Lichten, L. A., Samuelson, D. A., and Cousins, R. J. (2004) *Proc. Natl. Acad. Sci. U. S. A.* **101,** 14355–14360
7. Dufner-Beattie, J., Kuo, Y. M., Gitschier, J., and Andrews, G. K. (2004) *J. Biol. Chem.* **279,** 49082–49090
8. Kim, B. E., Wang, F., Dufner-Beattie, J., Andrews, G. K., Eide, D. J., and Petris, M. J. (2004) *J. Biol. Chem.* **279,** 4523–4530
9. Wang, F., Kim, B. E., Petris, M. J., and Eide, D. J. (2004) *J. Biol. Chem.* **279,** 51433–51441
10. Wang, F., Kim, B. E., Dufner-Beattie, J., Petris, M. J., Andrews, G., and Eide, D. J. (2004) *Hum. Mol. Genet* **13,** 563–571
11. Wang, F., Dufner-Beattie, J., Kim, B. E., Petris, M. J., Andrews, G., and Eide, D. J. (2004) *J. Biol. Chem.* **279,** 24631–24639
12. Dufner-Beattie, J., Langmade, S. J., Wang, F., Eide, D., and Andrews, G. K. (2003) *J. Biol. Chem.* **278,** 50142–50150
13. Gaither, L. A., and Eide, D. J. (2001) *J. Biol. Chem.* **276,** 22258–22264
14. Hicke, L. (1999) *Trends Cell Biol.* **9,** 107–112
15. Glickman, M. H., and Ciechanover, A. (2002) *Physiol. Rev.* **82,** 373–428
16. Welchman, R. L., Gordon, C., and Mayer, R. J. (2005) *Nat. Rev. Mol. Cell Biol.* **6,** 599–609
17. Schmid, S. L., McNiven, M. A., and De Camilli, P. (1998) *Curr. Opin. Cell Biol.* **10,** 504–512
18. Chau, V., Tobias, J. W., Bachmair, A., Marriott, D., Ecker, D. J., Gonda, D. K., and Varshavsky, A. (1989) *Science* **243,** 1576–1583
19. Finley, D., Sadis, S., Monia, B. P., Boucher, P., Ecker, D. J., Crooke, S. T., and Chau, V. (1994) *Mol. Cell Biol.* **14,** 5501–5509
20. Zhao, H., and Eide, D. (1996) *Proc. Natl. Acad. Sci. U. S. A.* **93,** 2454–2458
21. Gaither, L. A., and Eide, D. J. (2000) *J. Biol. Chem.* **275,** 5560–5564
22. Eng, B. H., Guerinot, M. L., Eide, D., and Saier, M. H., Jr. (1998) *J. Membr. Biol.* **166,** 1–7
23. Zhao, H., and Eide, D. (1996) *J. Biol. Chem.* **271,** 23203–23210
24. Eide, D., Broderius, M., Fett, J., and Guerinot, M. L. (1996) *Proc. Natl. Acad. Sci. U. S. A.* **93,** 5624–5628
25. Grotz, N., Fox, T., Connolly, E., Park, W., Guerinot, M. L., and Eide, D. (1998) *Proc. Natl. Acad. Sci. U. S. A.* **95,** 7220–7224
26. Karlin, S., and Zhu, Z. Y. (1997) *Proc. Natl. Acad. Sci. U. S. A.* **94,** 14231–14236
27. Longva, K. E., Blystad, F. D., Stang, E., Larsen, A. M., Johannessen, L. E., and Madshus, I. H. (2002) *J. Cell Biol.* **156,** 843–854
28. Levkowitz, G., Waterman, H., Zamir, E., Kam, Z., Oved, S., Langdon, W. Y., Beguinot, L., Geiger, B., and Yarden, Y. (1998) *Genes Dev.* **12,** 3663–3674
29. Yu, A., and Malek, T. R. (2001) *J. Biol. Chem.* **276,** 381–385
30. van Kerkhof, P., Alves dos Santos, C. M., Sachse, M., Klumperman, J., Bu, G., and Strous, G. J. (2001) *Mol. Biol. Cell* **12,** 2556–2566
31. Gitan, R. S., Luo, H., Rodgers, J., Broderius, M., and Eide, D. (1998) *J. Biol. Chem.* **273,** 28617–28624
32. Gitan, R. S., and Eide, D. J. (2000) *Biochem. J.* **346,** 329–336
33. Dalton, T. P., Bittel, D., and Andrews, G. K. (1997) *Mol. Cell Biol.* **17,** 2781–2789
34. Cao, J., Bobo, J. A., Liuzzi, J. P., and Cousins, R. J. (2001) *J. Leukoc. Biol.* **70,** 559–566
35. Huang, Z. L., Dufner-Beattie, J., and Andrews, G. K. (2006) *Dev. Biol.* **295,** 571–579

[4] X. Mao, B.-E. Kim, F. Wang, D. J. Eide, and M. J. Petris, manuscript in preparation.